Research Article

Received: 17 November 2023 Revised: 13 February 2024 Accepted article published: 19 February 2024 Published online in Wiley Online Library:

(wileyonlinelibrary.com) DOI 10.1002/jsfa.13407

Formulation of hesperidin-loaded *in situ* gel for ocular drug delivery: a comprehensive study

Sefa Gözcü,[a*] Heybet Kerem Polat,[b] Yakup Gültekin,[c] Sedat Ünal,[d] Nasıf Fatih Karakuyu,[e] Esra Köngül Şafak,[f] Osman Doğan,[g] Esra Pezik,[h] Muhammet Kerim Haydar,[h] Eren Aytekin,[g] Nihat Kurt[i] and Burak Batuhan Laçin[j]

Abstract

BACKGROUND: Allergic conjunctivitis is one of the most common eye disorders. Different drugs are used for its treatment. Hesperidin is an active substance isolated from *Citrus sinensis* L. (Rutaceae) fruit peels, with known anti-inflammatory activity but low solubility. It was complexed with cyclodextrin and encapsulated *in situ* gel to extend its duration in the eye.

RESULTS: The optimized formulation comprised 1% hesperidin, 1.5% hydroxyethyl cellulose, and 16% poloxamer 407. The viscosity at 25 °C was 492 ± 82 cP, and at 35 °C it was 8875 ± 248 cP, the pH was 7.01 ± 0.03, gelation temperature was 34 ± 1.3 °C, and gelation time was 33 ± 1.2 s. There was a 66% *in vitro* release in the initial 2 h, with a burst effect. A lipoxygenase (LOX) inhibition test determined that hesperidin was active at high doses on leukotyrens seen in the body in allergic diseases. In cell-culture studies, the hesperidin cyclodextrin complex loaded *in situ* gel, BRN9-CD (poloxamer 16%, hydroxy ethyl cellulose (HEC) 1.5%), enhanced cell viability in comparison with the hesperidin solution. It was determined that BRN9-CD did not cause any irritation in the ocular tissues in the Draize test.

CONCLUSION: The findings of this study demonstrate the potential of the *in situ* gel formulation of hesperidin in terms of ease of application and residence time on the ocular surface. Due to its notable LOX inhibition activity and positive outcomes in the *in vivo* Draize test, it appears promising for incorporation into pharmaceutical formulations.

Supporting information may be found in the online version of this article.

Keywords: hesperidin; cyclodextrin; cell viability; lox inhibition; Draize test

* *Correspondence to: Sefa Gözcü, Department of Pharmacognosy Faculty of Pharmacy Erzincan Binali Yıldırım University, 24100, Erzincan, Turkey. E-mail: sgozcu@erzincan.edu.tr*

a *Department of Pharmacognosy Faculty of Pharmacy, Erzincan Binali Yıldırım University, Erzincan, Turkey*

b *Republic of Turkey Ministry of Health, Turkish Medicines and Medical Devices Agency, Ankara, Turkey*

c *Department of Pharmaceutical Technology, Faculty of Pharmacy, Selcuk University, Konya, Turkey*

d *Department of Pharmaceutical Technology, Faculty of Pharmacy, Erciyes University, Kayseri, Turkey*

e *Department of Pharmacology, Faculty of Pharmacy, Suleyman Demirel University, Isparta, Turkey*

f *Department of Pharmacognosy, Faculty of Pharmacy, Erciyes University, Kayseri, Turkey*

g *Department of Pharmaceutical Technology, Faculty of Pharmacy, Hacettepe University, Ankara, Turkey*

h *Department of Pharmaceutical Technology, Faculty of Pharmacy, Erzincan Binali Yıldırım University, Erzincan, Turkey*

i *Department of Pharmaceutical Technology, Faculty of Pharmacy, Gaziosmanpasa University, Tokat, Turkey*

j *Department of Physiology, Faculty of Veterinary Medicine, Atatürk University, Erzurum, Turkey*

INTRODUCTION

Ocular allergy, a common manifestation of allergic disease, results from an inflammatory response within the ocular surface triggered by hypersensitivity reactions to environmental allergens. Characterized by itching, redness, tearing, and conjunctival swelling, allergic conjunctivitis represents a major subtype of ocular allergy. The pathophysiology of ocular allergy involves a complex immunological cascade initiated by allergen exposure.[1]

Ocular allergic disease is a term that refers to a variety of disorders that range in severity from mild to severe.[2] The initial encounter with allergens stimulates sensitization, producing allergen-specific immunoglobulin E (IgE) antibodies. Upon re-exposure, these antibodies bind to mast cells and basophils, triggering a release of inflammatory mediators like histamine.[3] Histamine plays a central role in promoting vasodilation, increasing vascular permeability, and stimulating nerve endings, contributing to the characteristic signs and symptoms of allergic conjunctivitis.[4,5]

The value of the worldwide market for eye pharmaceuticals was $29.2 billion in 2021 and is expected to reach $61.5 billion in 2032.[6] Ocular illnesses have a significant impact on patients' vision and quality of life. Globally, more than 250 million people are affected by vision impairment.[7] If there is no improvement in the treatment for blindness, it is projected that the 43.3 million cases worldwide estimated in 2020 could increase to nearly 115 million by 2050. This upward trend is related to the high population growth rates in underdeveloped countries and the aging of the global population.[8] This reinforces the need to highlight innovative drug delivery strategies to combat ocular diseases effectively.

According to the World Health Organization (WHO), the global market supports herbal medicinal products.[9] The use of complementary and alternative medicine has increased globally, according to studies conducted in the past decade.[10] It is thus important to create unique herbal-based solutions that are effective, nontoxic, and not harmful. Herbal medicine manufacture necessitates the processing of raw materials to obtain the required secondary metabolites. As a result, quality control is necessary to ensure that the processed raw materials remain functional. Manufacturers of herbal medicine must ensure the quality and effectiveness of all plant-based products.[11]

Citrus, the genus *Citrus* L. of the Rutaceae family, is one of the world's most important fruit crops. It is widely grown in tropical and subtropical regions of the world, as well as in many other locations, with an annual production of around 121 million tons.[12,13] Previously, various isolation and quantitative studies revealed the existence of bioflavonoid derivatives such as naringenin, naringin, hesperidin, hesperitin, and phenolic acids in *Citrus* fruits.[13] In health syndromes, bioflavonoids play an active role as free radical scavengers against reactive oxygen species.[14] The therapeutic efficacy of citrus bioflavonoids has been observed in addressing various conditions, including cancers,[15] neurodegenerative disorders,[16] cardiovascular diseases,[17] osteoporosis,[18] glaucoma,[19] inflammatory lung diseases,[20] and diabetes.[21] A recent article indicated potential anti-COVID-19 properties.[22,23] The existing literature has explored their antioxidant properties extensively but emerging research is shedding light on their anti-allergic properties, including notable effects in ocular manifestations.[14,24] Studies suggest that bioflavonoids may exert a protective influence against ocular allergic reactions by modulating inflammatory pathways and stabilizing mast cells. Moreover, the systemic impact of bioflavonoids on allergic responses in other tissues is increasingly recognized.[25,26] The ability of these compounds to inhibit histamine release and downregulate pro-inflammatory cytokines underscores their potential as novel candidates for the treatment of allergic disorders.[27,28] Further investigations into the specific mechanisms underlying bioflavonoids' interaction with allergic disease pathways are warranted to elucidate their therapeutic potential fully and pave the way for targeted interventions in diverse allergic conditions.[29]

Hesperidin is a flavanone with anti-inflammatory,[20] antioxidant, and anticancer[15] effects, which has proven effective against neurodegenerative disorders[16] and cardiovascular diseases,[17] and which also exhibits antiosteoporosis,[18] antiglaucoma,[19] antidiabetic,[21] and antibacterial effects.[11] Hesperidin has a strong pharmacological activity but is poorly soluble in water; therefore, several approaches have been employed to increase its solubility, including the use of liposomes, emulsions, and cyclodextrin complexes.[30] Making drug cyclodextrin complexes is one way to increase the solubility of lipophilic pharmaceuticals like hesperidin.

Cyclodextrins (CDs) are often used to augment the aqueous solubility of drugs with limited aqueous solubility and to increase corneal permeability. It has been determined that hesperidin-cyclodextrin inclusion complexes are formed by using β-CD.[31]

The eye's unique anatomical structures make it one of the organs to which it is hardest to administer drugs. Due to the eye's obstructions, drug delivery to the underlying tissue layers is challenging. Ninety percent of the ocular drugs currently on the market are contained in conventional eye drops. However, these eye drops have limitations, such as a brief residence time and rapid corneal evacuation through the ocular barriers.[32] Recently developed *in situ* gel drug delivery technologies are mostly used in ophthalmic formulations. Specific polymers that induce sol–gel phase transition by introducing environmental conditions like pH, specific ions, and temperature, are used in the preparation of *in situ* gels.[33,34] *In situ* gel formulations were first developed as liquids or suspensions, and then they were changed into gels to increase patient compliance. Studies have revealed that the corneal residence time of some *in situ* gel systems can reach several hours. Different polymers or polymeric combinations have been used to alter the release profile to meet needs.[35]

Poloxamer, a polymer utilized in *in situ* gel systems, possesses a thermoresponsive structure. Its amphiphilic behavior arises from the hydrophilic ethylene oxide and hydrophobic propylene oxide zones. Despite these advantageous properties, it is noteworthy that poloxamer lacks mucoadhesive qualities, representing a notable limitation. Other polymers, such as carbopol, hydroxy ethyl cellulose (HEC), and chitosan, have therefore been added to poloxamer-based ocular treatments to improve their mucoadhesive properties.[36] The main objective of this study is to increase hesperidin's solubility in CD. β-Cyclodextrin was used for this purpose. In accordance with the results of the phase-solubility experiment, a suitable CD was chosen to increase the solubility of hesperidin. Various proportions of poloxamer (between 12% and 20%) and HEC were examined for preparation of *in situ* gels.

In addition, developed gel formulations with hesperidin were evaluated in terms of clarity, pH, gelation temperature, rheological behaviors, *in vitro* release, release kinetics, cell viability, LOX inhibition studies, and *in vivo* Draize testing. Following the outcomes derived from *in vitro* characterization studies, a formulation deemed appropriate for ocular application was selected.

MATERIALS AND METHODS

Plant materials, extraction, and isolation of hesperidin

The fruits of *Citrus sinensis* L. (Rutaceae) were acquired from the local market in Erzincan, Turkey (Güneş Gross), and they were subsequently subjected to manual peeling. The peels were air-dried in a shaded environment.

Hesperidin was isolated using a Soxhlet apparatus (ISOLAB, Bayern, Germany) following the method described by Sharma *et al.*[37] The fruits of *C. sinensis* peel powder were first subjected to delipidation using petroleum ether (Merck, Darmstadt, Germany) (40–60 °C). The delipidated powder was then extracted with methanol (Merck, Darmstadt, Germany) until the solvent in the extraction sleeve became colorless, which typically took around 1 to 2 h. The resulting extract was evaporated using a rotary evaporator until it reached a syrup-like consistency. The residue obtained from the evaporation step was mixed with 50 mL of 6% acetic acid (Merck, Darmstadt, Germany), leading to the precipitation of crude hesperidin. The precipitated solid was separated using a Buechner funnel (ISOLAB, Bayern, Germany) and washed with 6% acetic acid (Merck, Darmstadt, Germany). For recrystallization, a 5% solution of the crude product in dimethyl formamide (Merck, Darmstadt, Germany) was prepared under continuous stirring and heating at 60–80 °C. Subsequently, the same volume of water was added slowly while stirring, and the mixture was cooled to room temperature, causing the precipitation of hesperidin. Crude hesperidin precipitated was eluted from a Sephadex (GE Healtycare, Chicago, USA) Column Chromatography (CC) with MeOH. The same procedure was repeated seven times and pure hesperidin was obtained (Fig. 1).

Identification of hesperidin

The hesperidin structure of the hesperidin obtained was compared with the literature[38] and it was identified using a spectral method 1D-NMR (one-dimensional nuclear magnetic resonance) (Varian Mercury Plus 400 MHz, Agilant, Mundelein, Illinois, USA). Sample was accurately weighed 20 mg and dissolved in 500-µL DMSO-d_6. ^{1}H and ^{13}C experiments were carried out using standard parameters. The nuclear magnetic resonance (NMR) probe head was set manually (400.13 MHz for ^{1}H and 100.61 MHz for ^{13}C) and all experiments were recorded at room temperature (23–25 °C).

Cyclodextrin-drug phase-solubility assay

(Phase-solubility study was carried out with the method developed by Loftson et al.[33] A constant amount of hesperidin was mixed with β-CD solution in increasing quantities (0–10 mM). A magnetic stirrer was used to agitate the resultant mixture for 7 days at room temperature. Afterwards, 0.45 µm membrane filters were used to filter all combinations containing hesperidin and β-CD. The ultraviolet-visible (UV-visible) spectrophotometer (UVmini-1240, Shimadzu, Kyoto, Japan) was used to measure the concentration of hesperidin in the supernatant at 405 nm.[39,40] The phase-solubility diagram was displayed at the conclusion of the investigation by comparing the concentration of β-CD with the amount of dissolved hesperidin. (Furthermore, the type of the obtained diagram was evaluated classification which includes A_P, A_L, A_N, B_S and B_I diagram models). Complex stability constant and complexation efficacy were calculated considering the equations defined elsewhere. The complex stability constant was calculated according to Eqn (1):[33]

$$complex\ stability\ constant = \frac{slope}{S0(1-slope)} \quad (1)$$

where S is the intrinsic hesperidine solubility, which is 7.5×10^{-6} mol L^{-1},[25] and Slope isthe slope of the linear regression of the phase-solubility diagram. The complexation efficacy was calculated according to Eqn (2)[39]

$$complexation\ efficacy = \frac{slope}{(1-slope)} \quad (2)$$

Freeze drying

Equal molar amounts of CD and hesperidin were weighed, and subsequently dissolved in methanol and water, respectively. After 24 h of stirring, the β-CD solution was dropped gradually into the hesperidin solution. Following the evaporation of methanol within 24 h, the resulting material was lyophilized.[41] To assess the inclusion complex, Fourier transform infrared spectroscopy (FTIR) and differential scanning calorimetry (DSC) were employed.

FTIR-ATR analysis

Chemical characterization of surfaces of plain (uncoated) or coated nanofiber insert formulations were performed using the attenuated total reflectance (ATR) FTIR attachment (FTIR-ATR).

Differential scanning calorimetry

Differential scanning calorimetry analyses were performed on HP-β-CD-BH inclusion complexes and BH:CD physical mixtures with a DuPont DSC 910 instrument (DuPont, Wilmington, Delaware, USA) differential scanning calorimeter. Samples weighing approximately 3 mg were heated in hermetically sealed aluminum pans

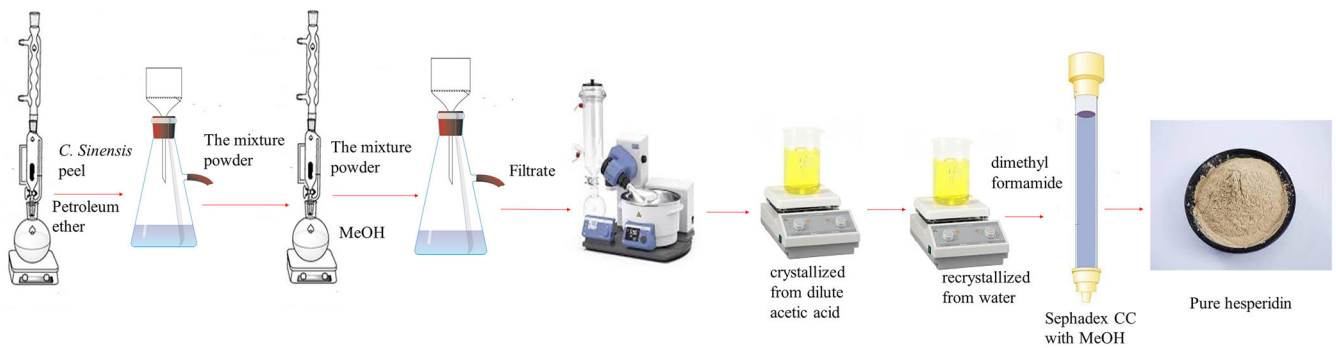

Figure 1. Hesperidin extraction and isolation scheme.

Table 1. Composition of formulations for *in situ* gel production

Code	Hesperidin or Hesperidin: CD (%)	Poloxamer (%)	HEC (%)	BAC (%)	NaCl (%)	Water
BRN1	1	12	0.5	0.001	0.2	100
BRN2	1	12	1	0.001	0.2	100
BRN3	1	12	1.5	0.001	0.2	100
BRN4	1	14	0.5	0.001	0.2	100
BRN5	1	14	1	0.001	0.2	100
BRN6	1	14	1.5	0.001	0.2	100
BRN7	1	16	0.5	0.001	0.2	100
BRN8	1	16	1	0.001	0.2	100
BRN9	1	16	1.5	0.001	0.2	100
BRN10	1	18	0.5	0.001	0.2	100
BRN11	1	18	1	0.001	0.2	100
BRN12	1	18	1.5	0.001	0.2	100
BRN13	1	20	0.5	0.001	0.2	100
BRN14	1	20	1	0.001	0.2	100
BRN15	1	20	1.5	0.001	0.2	100

Abbreviations: CD, cyclodextrins; BAC, benzalkonium chloride; HEC, hydroxy ethyl cellulose.

at a rate of 10 °C/min, between 25 and 300 °C in a dynamic nitrogen atmosphere.

In situ gel production

Hesperidin's *in situ* gel was created using the cold technique. This method was carried out by dispersing a certain volume of poloxamer 407 (12–20%) in distilled water and adding hydroxy ethyl cellulose (HEC) (1–1.5–0.5%). Then all solutions were cooled at 4 °C, overnight. Prior to use, each sample was kept at 4 °C. Hesperidin or hesperidin:CD, NaCl and benzalkonium chloride (BAC) were added (Table 1).

In vitro characterization of *in situ* gel

A pH meter (Hanna, Vöhringen, Germany) was used to measure the pH. Three measurements in total were taken ($n = 3$). Holding the *in situ* gel formulation up to bright light and comparing it with a dark background allowed us to evaluate the clarity of the formulation after gelation. To measure gelation temperature, the polymer solution was stirred in a water bath using a magnetic stirrer (Thermomac-TM19). The polymer solutions were heated at 100 rpm and 1 °C/min while being stirred.[42] To determine gelation time, a test tube containing 2 mL of the sample held at 4 °C was placed in a water bath that had been heated to the gelation temperature (35 °C). The *in situ* gel was periodically turned upside down to check for gelation. The gelation time was recorded when no flow of the gel was observed during tube inversion.[43] To measure viscosity, Fungilab rotating viscometer (Hauppauge, New York, USA) samples were tested for viscosity at 10 rpm using an R5 spindle. All hesperidin-loaded *in situ* gels had their viscosity values tested at both 25 and 37 °C.[43] The rheological characteristics of the samples were assessed utilizing a rotating viscometer made by Fungilab with an R5 spindle rotating at various speeds (1, 2.5, 5, 10, 20, and 50 rpm). Viscosities were measured at various angular velocities to compute the flow curves.[31]

Stability assay

After 3 months of storage (25 °C), the effects on pH, gelation temperature, and viscosity were seen and recorded.[44]

In vitro release from *in situ* gel

The dialysis bag technique was used to complete the *in vitro* release research. Following that, the dialysis membrane (Sigma, D9277) was sealed, 100 µL of *in situ* gel was added, and 10 mL of an isotonic phosphate buffer with a pH of 7.4 at 35 °C was added. All the media were removed at different periods, and 10 mL of the new buffer media were introduced (0, 1, 2, 4, and 8 h). The amount of hesperidin released was measured using a UV-visible spectrophotometer.

Release kinetic assay

Utilizing DDSolver Software, it was possible to identify the mathematical models associated with formulations.[45] Models of formulation release kinetics were examined using information from *in vitro* release investigations. To this end, four different parameters, R^2, R^2_{adj}, the model selection criterion (MSC), and the Akaike information criterion (AIC), were selected and the model with the highest R^2, R^2_{adj}, MSC, and the lowest AIC was chosen as the best fitted mathematical model for formulations.[46]

In vitro cytotoxicity assay

Ocular formulations were employed using L929 (mouse fibroblast) cells (ATCC, Rockville, MD, USA).[47,48] In this experiment, L929 (mouse fibroblast) cells (passage number: 22) were grown at 37 °C in a humidified incubator with 5% CO_2 and 10% fetal bovine serum (FBS) (Biochrom AG, Berlin, Germany), 50 U mL^{-1} penicillin, and 50 µg mL^{-1} streptomycin (Biochrom AG) added to Dulbecco's Modified Eagle's Medium (DMEM) (Biochrom AG). Cells were seeded at a density of 50 000 cells per milliliter (5000 cells per well) on a 96-well plate following cell counting with the Thoma slide counting chamber. Well contents were extracted during an overnight incubation. Cells were exposed to *in situ* gels containing hesperidin at doses of 1.56, 6.25, 25, 100, and 400 µg/mL. Hesperidin *in situ* gel stock solutions were produced in dimethyl sulfoxide (DMSO) (Applichem, Germany), and dilutions were made using the entire medium. Blank *in situ* gel stock solutions were created in DMEM, and dilutions were made using the entire medium. Following the delivery of the medication and *in*

Journal of The Science of Food and Agriculture published by John Wiley & Sons Ltd on behalf of Society of Chemical Industry.

situ gel, cells were allowed to rest for 2 h before receiving 25 μL of MTT solution (5 mg/mL) and continuing to incubate for a further 4 h. After that, each well received 200 μL of DMSO, and the microplate reader (BiotEKM Synergy HT, USA) was used to measure the absorbance levels.

Lipoxygenase (LOX) assay

The modified Waslidge and Hayes technique for the lipoxygenase test was used in 96-well microplates.[49] An aliquot of 50 μL of LOX (Sigma, L6632) in 50 mM Tris HCl buffer, pH 7.4 (final concentration, 100 ng protein/mL), and 20 μL of sample were incubated at 25 °C for 5 min. As a control, 20 μL of buffer containing 50 μL of LOX solution and 0.2% v/v DMSO (final concentration) was used. The reaction was started by adding 50 μL of linoleic acid (final concentration, 140°M) in 50 mM Tris HCl buffer, pH 7.4. The reaction mixture was incubated at 25 °C for 20 min in the dark. The experiment was terminated by adding 100 μL of freshly prepared ferrous oxidation-xylenol orange (FOX) reagent (sulfuric acid (30 mM), xylenol orange (100 μM), iron (II) sulfate (100 μM), methanol/water (9:1). It was then treated with Fe^{3+}–dye complex for 30 min at 25 °C. Absorbances were measured at 560 nm in a microplate reader (BiotEKM Synergy HT, Santa Clara, USA).[50] The percentage enzyme inhibitions of the samples were calculated using Eqn (3);

$$inhibition\% = [(Abscontrol - Abssample)/Abscontrol] \times 100 \quad (3)$$

In vivo Draize test

The institutional review board and ethics committees of Suleyman Demirel University accepted the animal protocol, which complied with the Association for Research in Vision and Ophthalmology Statement for the Use of Animals in Ophthalmic Vision and Research.

Six adult male Wistar albino rats, weighing 390–530 g were used in this study. The animals were kept in a room with free access to food and water, a 12 h light cycle, and a constant temperature of 22 °C. All rats were given intramuscular injections of 5.0 mg/kg xylazine hydrochloride (Rompun; Bayer, Istanbul, Turkey) and 50 mg/kg ketamine hydrochloride (Ketalar; Eczacbaş, Istanbul, Turkey) to induce anesthesia. The Draize-derived ocular irritation score system (Supporting Information, Table S1) criteria and a slit lamp examination were used to evaluate the ocular surface.[51,52] The BRN9-CD formulation to be used in the *in vivo* study was kept under UV light (254 nm) for 24 h.[53] Every 30 min for 6 hours, BRN9-CD (50 mL) was topically applied in the left eye (12 treatments). Right eyes were used as controls and were given distilled water treatment. To assess the ocular tissues, three observations were made at 10 min, 6 h, and 24 h following the last treatment. Conjunctival congestion, swelling, discharge, and redness were assessed on a scale of 0 to 3, 0 to 4, 0 to 3, and 0 to 3, respectively, while corneal opacity and irritation were graded on a scale of 0 to 4 and 0 to 3, respectively.[54]

Histological examination

The corneas were removed immediately for histological investigation and stored in 10% formaldehyde. After fixation, the specimens were placed into designated cassettes and dried serially in increasing amounts of alcohol before being cleaned in xylene. Each cornea was then split in half and embedded in paraffin after this process (Leica EC Embedding Center, Wetzlar, Germany). Sections of 5 μm thickness were cut out of paraffin-embedded corneas. After an overnight deparaffinization process, sections were treated with xylene and dehydrated for 30 min in successive alcohols. The sections were subsequently stained with H&E and inspected under a light microscope (Leica DMR, Leica Microsystems GmbH, Wetzlar, Germany).

RESULTS

Identification of hesperidin by NMR

Hesperidin was isolated from *C. sinensis* fruit peel and was identified by 1D-NMR (Fig. 2(a),(b)). In the ^{1}H-NMR spectrum (Fig. 2) a broad singlet at δ 12.03 ppm corresponds to the hydroxyl group proton at 5-OH. H-2′ is a doublet at δ 6.91 ppm and J = 2.0 Hz. H-5′ is a singlet at δ 6.89 ppm. H-6′ is a doublet of doublets at δ 6.95 ppm with J values of 8.0 and 2.0 Hz. H-8 is a singlet at δ 6.15 ppm with J = 2.0 Hz. H-6 is a doublet at δ 6.13 ppm with J = 2.0 Hz. A doublet of doublets at δ 5.50 ppm (J = 11.0, 5.0 Hz) corresponds to H-2. H-1″ is a doublet at δ 4.97 ppm with J = 7.2 Hz. A broad singlet at δ 4.53 ppm corresponds to H-1″. OCH_3 are a singlet at δ 3.77 ppm. The region between δ 3.15 and 3.63 ppm includes multiplets for protons H-2″ to H-6″ (six protons) and H-2 to H-6 (three protons), indicating methylene

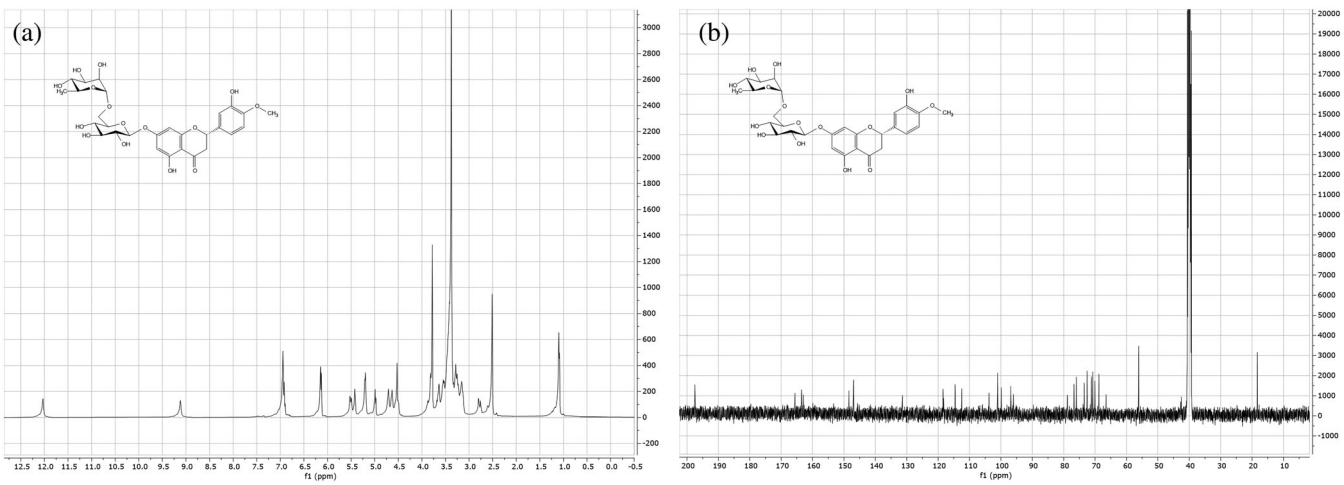

Figure 2. (a, b) Spectrum 1 Hydrogen- nuclear magnetic resonance (^{1}H-NMR) and 13 Carbon-nuclear magnetic resonance (^{13}C-NMR) of hesperidin.

Table 2. H^1 and C^{13} nuclear magnetic resonance (NMR) chemical shift assignments for hesperidin

No	^1H	^{13}C
2	5.50 (dd)	78.9 (CH)
3	3.14 (dd), 2.77 (dd)	42.5 (CH_2)
4	-	197.5 (C)
5	-	163.1 (C)
6	6.13 (d)	96.1 (CH)
7	-	165.3 (C)
8	6.15 (d)	96.9 (CH)
9	-	162.8 (C)
10	-	103.9 (C)
1′	-	130.8 (C)
2′	6.91 (bs)	118.5 (CH)
3′	-	146.9 (C)
4′	-	148.4 (C)
5′	6.89 (bs)	112.3 (CH)
6′	6.95 (bs)	114.8 (CH)
O-CH_3	3.77 (s)	56.1 (CH_3)
1″	4.97 (d)	100.1 (CH)
2″	3.15–3.63 (m)	73.4 (CH)
3″	3.15–3.63 (m)	76.1 (CH)
4″	3.15–3.63 (m)	70.7 (CH)
5″	3.15–3.63 (m)	76.8 (CH)
6″	3.41-3.80	66.5 (CH_2)
1‴	4.53 (bs)	101.1 (CH)
2‴	3.15–3.63 (m)	71.3 (CH)
3‴′	3.15–3.63 (m)	70.1 (CH)
4‴	3.15–3.63 (m)	72.6 (CH)
5‴	3.15–3.63 (m)	68.7 (CH)
6‴	1.09	17.9 (CH_3)

groups. H-3a and H-3b are a multiplet at δ 3.14 ppm, δ 2.77 ppm, respectively. The methyl protons form a triplet at δ 1.09 ppm. In the ^{13}C NMR spectrum (Fig. 2(b)), The carbonyl carbon resonated at 197.5 ppm (C-4) and the shift of C-5 to 163.1 ppm proves that this OH group is attached to this carbon. The value of 100.07 ppm of C-1′ anomeric carbon shows that it is bonded to more than one electronegative oxygen. Diastereotopic protons at the C-6″ (66.5 ppm) carbon indicate the presence of two glycoside groups bonded in the structure (Table 2). The isolated compound's structure was identified as hesperidin after comparing the results with those reported in the literature.[38,55]

Cyclodextrin-drug phase-solubility assay

The results of the phase solubility study are given in Fig. 3. The results of FTIR and DSC studies conducted to evaluate the complexes are shown in Fig. 4 and Fig. 5, respectively. Phase-solubility studies are the method used most frequently to assess how drug-CD complexation affects drug solubility.[56] The most common type of association that occurs when a drug molecule is integrated into a CD molecule's cavity is called a 1:1 drug/CD inclusion complex, which has a stability constant of K1:1 for the condition of equilibrium between free and related species. Examining the solubility graphs indicated that β-CD shows a linear rise (Fig. 3). The decision was made to label the β-CD diagram as 'AL-type' in accordance with the phase-solubility diagram; for this reason, it was used at a ratio of 1 mM:1 mM while preparing the hesperidin:CD

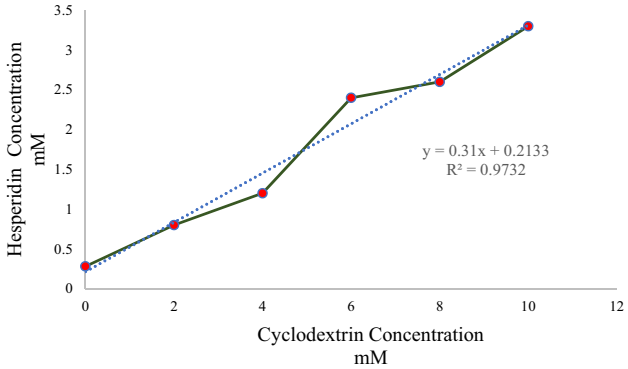

Figure 3. Phase-solubility diagram of hesperidin at the increasing β-CD (n = 3; means ± SDs). CD, cyclodextrins.

complex. By examining the β-CD straight line (r^2 = 0.9732), calculated values for the β-CD's complexity efficiency (CE) and stability constant (Ks) are 0.44 and 5941 M^{-1}, respectively. According to the literature, a Ks value of 100 to 10 000 M^{-1} is appropriate for creating the drug:CD complex.[41]

In vitro gel characterization

The pH of *in situ* gel compositions was found to range between 6.78 ± 0.04 to 7.02 ± 0.01 (Table 3). The formulations' gelling characteristics are displayed in Table 3. Under non-physiological (4 °C) and physiological (35 °C) circumstances, the lowest polymer-containing samples, BRN1, BRN2, and BRN3 (12% poloxamer), displayed a sol (liquid) state without gelation, demonstrating that they could not gel. Samples should immediately or quickly gel when brought up to the system's gelation temperature to stop tear fluid from fast evaporating.[57] Gelation was not observed in BRN1, BRN2, and BRN3. The gelation times for BRN4 and BRN15 were around 41 ± 1.2 and 23 ± 1.5 s, respectively (Table 3).

As a result of *in vitro* characterization studies, BRN9 was found to be more suitable for ocular application. This selected formulation was loaded with hesperidin (BRN9) and hesperidin-β-CD inclusion complex (BRN9-CD). The necessary measurements of these drug-loaded formulations were made (Supporting Information, Table S2). It was determined that there was no change in the parameters of the formulations depending on the drug loading.

Rheology, viscosity, stability, and drug-release assay

Figure 6 presents the viscosity data for *in situ* gelling systems at various shear rates. There were no significant changes in viscosity, gelation temperature, or pH when the stability data were analyzed, and it was determined that they were suitable for ocular usage for all values (Supporting Information, Table S3). *In situ* gel was employed to examine the drug release *in vitro* at a temperature of 35 °C in an isotonic phosphate buffer, and all formulations contained hesperidin (0.1% w/v). Figure 7(a) shows the features of *in vitro* drug release.

Release kinetic assay

As shown in Table 4, Korsmeyer-Peppas is the best-fitted model for BRN9. The BRN9-CD formulation shows consistency with the Baker–Lonsdale model. Supporting Information, Table S4 illustrates the similarity (f2) and difference factor (f1) between two formulations.

Journal of The Science of Food and Agriculture published by John Wiley & Sons Ltd on behalf of Society of Chemical Industry.

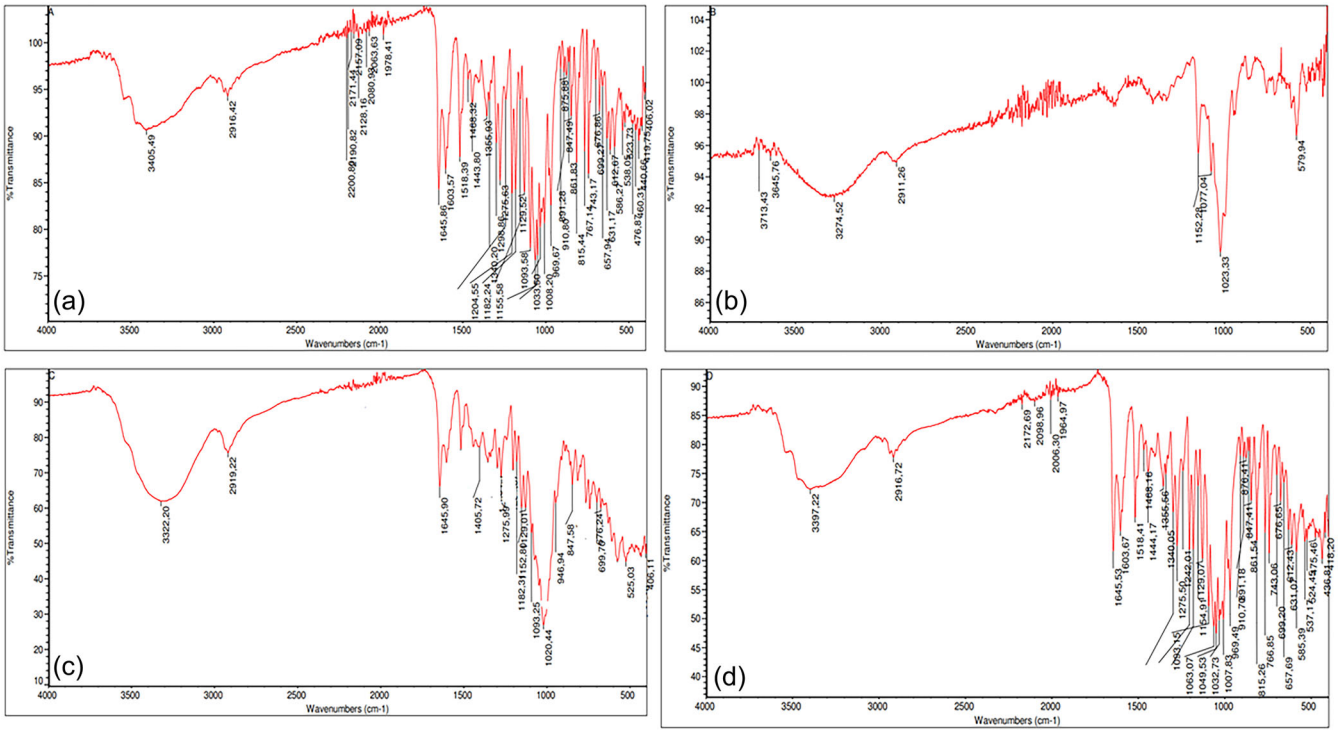

Figure 4. Fourier transform infrared spectroscopy (FTIR) spectra of A (hesperidin), B (*β*-CD), C (hesperidin-CD inclusion complex), D (hesperidin-CD physical mix).

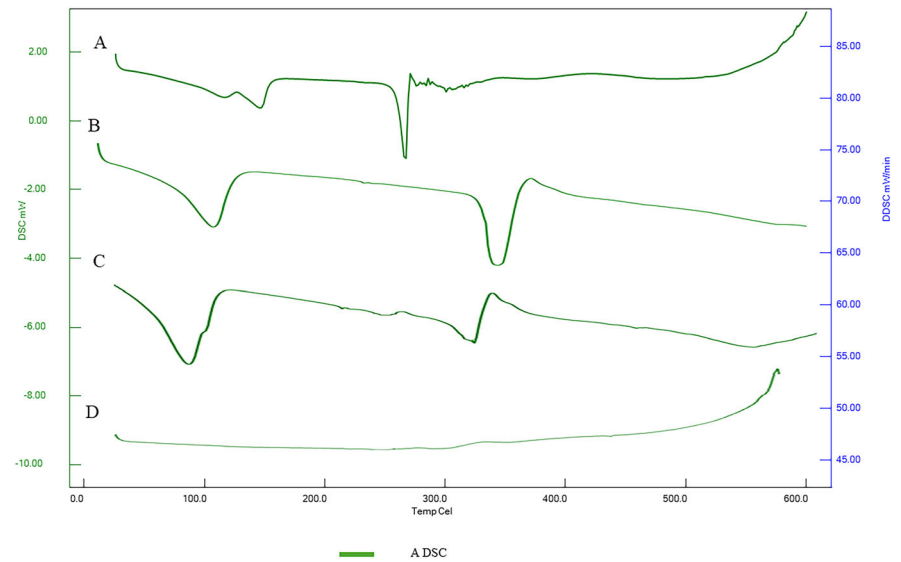

Figure 5. Differential scanning calorimetry (DSC) thermogram of A (hesperidin), B (*β*-CD), C (hesperidin-CD physical mix), D (hesperidin-CD inclusion complex).

In vitro cytotoxicity assay

The biocompatibility of the *in situ* gel was investigated by MTT assay using L929 cells. Figure 7(b) showed that the cytotoxicity of L929 was present. Cell viability was observed to be higher with in situ hesperidin loading than with hesperidin at all dosages. For BRN9 and BRN9-CD, the cell viability at 400 g/mL was 110% and 113%, respectively. Hesperidin-loaded gels and hesperidin solutions differ statistically significantly ($P < 0.01$).

Lipoxygenase inhibition assay

The inhibitory activity of hesperidin and hesperidin-CD complex on lipoxygenase enzyme was investigated by the Ferrous Oxidation-Xylenol Orange (FOX) assay. It has been studied at concentrations of 1.67–0.001 mg/mL. For phenidone used as a positive control, the IC_{50} was found to be 3.26 ± 0.21 µg/mL, whereas hesperidin did not show inhibitory activity at any dose. However, the hesperidin-CD complex caused a 39.4% decrease in enzyme activity at the highest dose (Fig. 7(c)).

Journal of The Science of Food and Agriculture published by John Wiley & Sons Ltd on behalf of Society of Chemical Industry.

Table 3. Results of *in vitro* characterization of *in situ* gels ($n = 3$; means ± SDs)

Code	Viscosity 25 °C	Viscosity 35 °C	pH	Geltaion Temprature(°C)	Gelation Time (s)	Clarity
BRN1	193 ± 32	298 ± 45	713 ± 0.02	No Gelation	No Gelation	Clear
BRN2	175 ± 28	327 ± 61	7.04 ± 0.01	No Gelation	No Gelation	Clear
BRN3	217 ± 24	389 ± 44	7.03 ± 0.07	No Gelation	No Gelation	Clear
BRN4	208 ± 47	367 ± 41	7.09 ± 0.05	41 ± 1.2	56 ± 1.5	Clear
BRN5	254 ± 31	527 ± 71	7.03 ± 0.04	39 ± 1.85	52 ± 1.9	Clear
BRN6	298 ± 42	584 ± 65	7.02 ± 0.06	39 ± 0.9	50 ± 1.3	Clear
BRN7	319 ± 53	2875 ± 246	7.07 ± 0.08	37 ± 1.1	42 ± 1.6	Clear
BRN8	412 ± 71	3125 ± 321	7.06 ± 0.04	36 ± 0.94	39 ± 2.4	Clear
BRN9	492 ± 82	8875 ± 248	7.01 ± 0.03	34 ± 1.3	33 ± 1.2	Clear
BRN10	548 ± 99	10 247 ± 449	7.1 ± 0.04	32 ± 1.08	30 ± 1.1	Clear
BRN11	594 ± 107	10 374 ± 430	7.02 ± 0.09	32 ± 1.4	29 ± 1.3	Clear
BRN12	694 ± 228	14 846 ± 523	6.99 ± 0.1	30 ± 1.10	27 ± 1.4	Clear
BRN13	1197 ± 129	18 756 ± 620	7.02 ± 0.05	26 ± 1.3	22 ± 1.1	Clear
BRN14	8198 ± 325	22 845 ± 553	7 ± 0.1	25 ± 1.12	19 ± 0.9	Clear
BRN15	18 451 ± 31	25 923 ± 741	6.97 ± 0.07	23 ± 1.5	18 ± 0.7	Clear

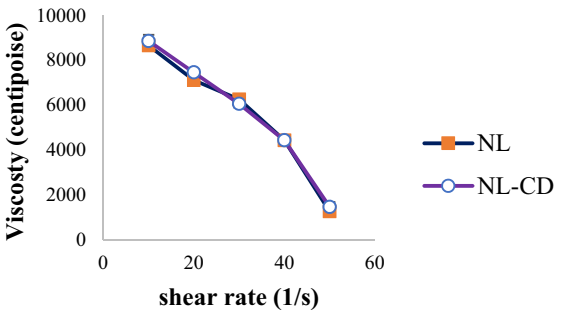

Figure 6. *In situ* gelling systems' rheological characteristics ($n = 3$; means ± SDs).

In vivo Draize test

Regardless of the time at which the degree of irritation was recorded, there was no difference between the control solution and *in situ* gel in terms of the degree of irritation on the cornea and conjunctiva (Figs 7(d) and 8).

Histological studies

The control and BRN9-CD groups displayed normal histological characteristics during the histological investigation. Microscopically, no anomalous discoveries were found (Fig. 9). The corneal epithelium was found to be in normal alignment in both groups, the stroma was made up of normal collagen structures, and Descemet's membrane was made up of normal cells.

DISCUSSION

Initially, hesperidin was isolated from *C. sinensis*, and its structure was elucidated. The stretching vibration of the carbonyl in hesperidin's spectrum was matched by a prominent absorption band at 1644 cm^{-1}. This typical carbonyl stretching vibration was substantially wider and moved to a value of 1652 cm^{-1} in the complex, pointing to the creation of the complex (Fig. 4). In Fig. 5, the DSC thermograms are indicated. The DSC scans of pure hesperidin showed an endothermic peak at 259 °C, which is the melting temperature of the substance. However, the complex, which was produced by combining both chemicals and letting them dissolve in methanol (1:1 mol L^{-1} ratio) before allowing the mixture to evaporate, did not exhibit the peak. In light of this, it is strongly suggested from the combined chemical, thermal, and spectroscopic evidence that an inclusion complex evolved.[30]

A review of the literature indicates that ocular applications are suitable for the pH range of 4 to 8.[58] Hence, considering the findings, it can be concluded that each formulation is suitable for ocular delivery. Precise formulations are required for ocular applications. Even when drug delivery methods like ointments are effective, patient compliance is low because they impair vision. Whatever the drug's effectiveness, the required outcomes will not be achieved if the patient does not follow instructions. As a result, for compositions meant for use in eyes, transparent materials are needed.[58]

Ophthalmic thermoreversible gels have a sol–gel transition temperature range of 25 to 34 °C, making them acceptable for ocular delivery. When the gelation temperature of the thermosensitive formulation is lower than 25 °C, a gel may form at room temperature. When the temperature rises above 34 °C, a liquid dosage form stays at ocular surface temperature, causing the formulation to drain from the eyes.[36] Systems with different concentrations of poloxamer and different amounts of HEC were created and tested for gelling capacity to find the best mixtures to use as *in situ* gels. These findings show that the thermosensitivity and gelation speed of poloxamer gel was strongly concentration dependent; a higher poloxamer concentration sped up gelation at a lower gelation temperature. In order to decrease the *in situ* gel's polymer concentration while enhancing its gelling properties and rheological behavior, the interaction of an *in situ* gelling polymer with HEC as a viscosity modifying agent was examined. The ideal gelation temperature was found in BRN9 (16% poloxamer and 1.5% HEC).

It should gel immediately or quickly when brought up to the system's gelation temperature to stop tear fluid from evaporating quickly.[57] BRN15, which had more significant concentrations of poloxamer and HEC, also required less gelation time. According to this research, greater poloxamer and HEC concentrations led to shorter gelation periods and lower effective sol–gel transition temperatures.[43]

Journal of The Science of Food and Agriculture published by John Wiley & Sons Ltd on behalf of Society of Chemical Industry.

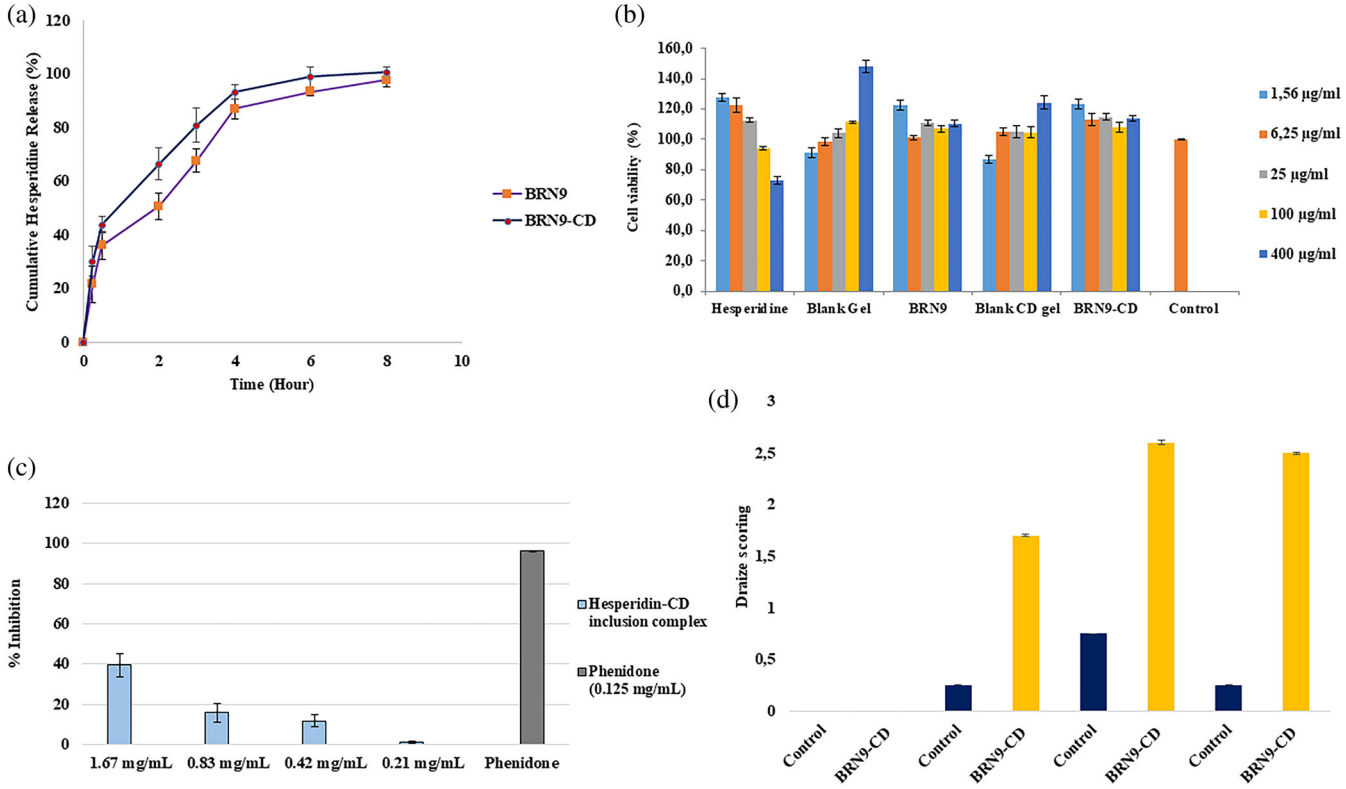

Figure 7. (a) *In vitro* release profiles of hesperidin ($n = 3$; mean ± SD), (b) The biocompatibility of the hesperidin, blank gel, BRN9 gel, CD blank gel, BRN9-CD gel and control were investigated by MTT assay using L929 (mouse fibroblast) cells ($n = 3$; means ± SDs) (c) percentage inhibitory effect of hesperidin-CD inclusion complex on lipoxygenase (LOX) enzyme at different concentrations. Phenidone at a dose of 0.125 mg/mL was used as a positive control, ($n = 3$; means ± SDs) (d) Draize test evaluation ($n = 3$; mean ± SD).

Table 4. Mathematical model results for BRN9 and BRN9-CD

Model and equation/Formulation		Evaluation criteria						
		Parameters		R^2	$R^2_{adjusted}$	AIC	MSC	n/m*
Zero-order	BRN9	k0	15 612	0.6353	0.6353	667 460	0.3132	-
$F = k0*t$	BRN9-CD	k0	16 833	0.3831	0.3831	712 794	-0.3505	-
First-order	BRN9	k1	0.447	0.9441	0.9441	517 468	21 880	-
$F = 100*[1-Exp(-k1*t)]$	BRN9-CD	k1	0.723	0.9432	0.9432	521 995	20 345	-
Higuchi	BRN9	kH	38 097	0.9644	0.9644	481 267	26 406	-
$F = kH*t^{0.5}$	BRN9-CD	kH	41 840	0.9110	0.9110	557 920	15 855	-
Korsmeyer–Peppas	BRN9	kKP	43 571	0.9780	0.9743	462 902	28 701	0.413
$F = kKP*t^n$	BRN9-CD	kKP	54 601	0.9855	0.9831	432 767	31 499	0.325
Hopfenberg	BRN9	kHB	0.000	0.9440	0.9347	537 508	19 376	1028.915
$F = 100*[1 - (1 - kHB*t)^n]$	BRN9-CD	kHB	0.000	0.9432	0.9337	542 011	17 843	7560.950
Baker–Lonsdale	BRN9	kBL	0.045	0.9756	0.9756	451 269	30 155	-
$3/2*[1 - (1 - F/100)^{(2/3)}] - F/100 = kBL*t$	BRN9-CD	kBL	0.063	0.9921	0.9921	364 416	40 043	-
Peppas–Sahlin	BRN9	k1	48 193	0.9800	0.9721	475 024	27 186	0.527
$F = k1*t_m + k2*t^{(2*m)}$	BRN9-CD	k1	65 293	0.9941	0.9918	380 202	38 069	0.492
Weibull	BRN9	β	0.743	0.9671	0.9539	515 013	22 187	-
$F = 100*1 - Exp[-((t-Ti)^{\beta})/\alpha]$	BRN9-CD	β	0.674	0.9856	0.9799	451 971	29 098	-

In all models, F is the fraction (%) of drug released in time t, k0: zero-order release constant, k1: first-order release constant, kH: Higuchi release constant, kHC: Hixson-Crowell release constant, kKP: release constant incorporating structural and geometric characteristics of the drug-dosage form, kHB: Hopfenberg release constant, n: is the diffusional exponent indicating the drug-release mechanism, m: diffusional exponent and similar exponent like n, m use in Peppas-Sahlin model equation only, α: is the scale parameter which defines the time scale of the process; β: is the shape parameter which characterizes the curve as either exponential (β=1; case 1), sigmoid, S-shaped, with upward curvature followed by a turning point ($\beta > 1$; case 2), or parabolic, with a higher initial slope and after that consistent with the exponential ($\beta < 1$; case 3), Ti: is the location parameter which represents the lag time before the onset of the dissolution or release process and in most cases will be near zero.

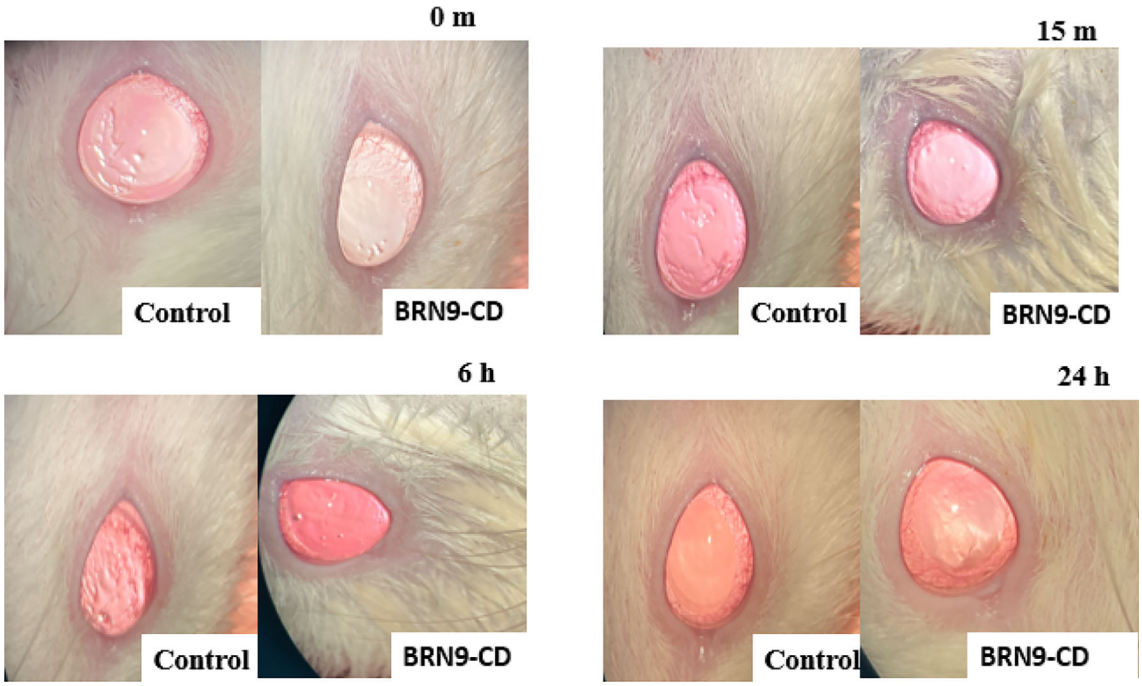

Figure 8. Results from eye irritation studies of *in situ* gel.

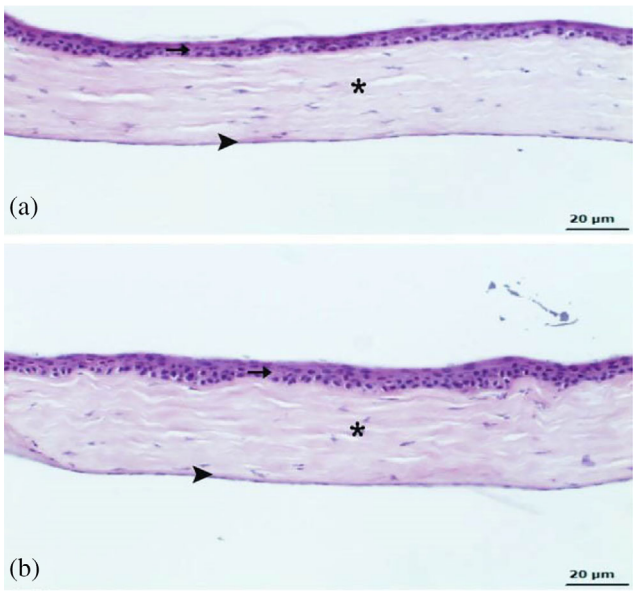

Figure 9. (a) Control group, (b) BRN9-CD group, normal appearance corneal epithelium (arrow), stroma (*) and Descemet's membrane. Scale bar represents 20 µm.

Table 3 shows the results of the rheology studies. According to a review of the literature, a viscosity between 50 and 50 000 cp is suitable for the best ocular delivery.[42] As the formulation stays in the cul-de-sac area of the eye for a longer period, the bioavailability will increase according to the increase in viscosity. Measurements were taken at 25 and 35 °C, and at 10 rpm, to determine the viscosity values for each formulation. The data analysis revealed that the viscosity values varied according to the polymer concentrations. This clearly illustrates the importance of the connection between polymer content and viscosity. Upon comparing the data with information available in the literature, it was observed that our results were consistent.[42]

When they began to gel, all the developed formulations exhibited shear-thinning flow characteristics (Fig. 6). However, when employing low-viscosity *in situ* gels, tears would easily wash them away from the surface of the eye. Issues may arise when utilizing *in situ* gels that are excessively viscous. High-viscosity ocular formulations ought to be avoided since they frequently leave an obvious residue on the side of the eyelid where they are applied. By employing *in situ* gel formulations with pseudo-plastic behavior, it is feasible to reduce the detrimental effects of ocular reflexes, like blinking, on the formulation. The pseudo-plastic flow of the formulation makes application more enjoyable and prolongs corneal contact time.[59] When the literature was examined, it was found that there were similar results for *in situ* gel formulations.[60,61]

In release studies, BRN9 indicated a drug release of more than 50% after 2 h and 67% after 3 h. Cyclodextrin was a component of the formulation, and BRN9-CD showed more than 66% drug release after 2 h. *In vitro*, release tests showed that the BRN9-CD formulation released more quickly than the BRN9 formulation because of the hesperidin-CD inclusion complex in the BRN9-CD formulation. The development of drug-CD increased the drug's solubility, which in this instance significantly affected the release time. When the literature was examined, comparable findings were found. Examples include formulations for inserts containing besifloxacin HCl and besifloxacin HCl-CD inclusion complex as a consequence of Polat *et al.*'s research.[56] According to the findings of the release studies, the drug-CD complex formulation with an insert had a higher release rate than the drug alone.[56] A different study created two distinct thermosensitive *in situ* gel formulations with dexamethasone and dexamethasone CD inclusion complex. Following the release trials, the burst effect was enhanced by enhancing resolution with the inclusion complex.[31] Sharif *et al.* reported that the electrospinning of HP-β-CD-drug inclusion

Journal of The Science of Food and Agriculture published by John Wiley & Sons Ltd on behalf of Society of Chemical Industry.

complexes produced a structure with a greater burst effect than those made with free drug.[62]

When the *n* value (the release exponent for Korsmeyer-Peppas) is examined, it is lower than 0.43, which means that drug molecules are liberated from nanoparticles by Fickian diffusion.[63] Formulations with f1 values less than 15 and f2 value higher than 50 have similar release profiles.[64] f1 and f2 results revealed that BRN9 and BRN9-CD formulations exert similar release profiles.

Recently, there have been advances in drug delivery systems Accordingly, the importance of controlled-release dosage forms has attracted attention. Drug molecules released from nanosystems exert different profiles including simple diffusion, erosion, and degradation, which play a vital role in determining the fate of drugs in target tissue. Modeling of the release kinetics of formulations therefore brings many advantages.[65] For this purpose, in this study, DDSolver software was used to predict the release kinetic models of formulations. DDSolver facilitates the prediction of mathematical modeling studies with lower margins of error. Within the scope of the modeling studies of formulations, eight models (zero order, first order, Higuchi, Korsmeyer–Peppas, Peppas–Sahlin, Hopfenberg, Weibull, and Baker–Lonsdale) were investigated. Similarity and difference factors that helped to determine the similarity between the two formulations were also evaluated. Each of the release models evaluated in release kinetic studies represents different release mechanisms. A formulation can sometimes be mathematically compatible with only one model but sometimes it can be seen to be compatible with more than one model.[66] This also shows that *in vitro* releases from formulations are related to different mechanisms and processes. Among the formulations within the scope of the study, BRN9 was found to be compatible with the Korsmeyer–Peppas model, while BRN9-CD was found to be compatible with the Baker–Lonsdale model.

In the Korsmeyer–Peppas model, *n* stands in for the diffusional exponent showing the drug release mechanism. In this context, *n* diffusional exponent values were computed as 0.413. If the diffusional exponent (*n*) is 0.45 or less, drug release depends on Fickian diffusion. For $0.45 < n < 0.85$, the drug release occurs through a non-Fickian diffusion mechanism; for $n = 0.85$ the release occurs by case II transport and $n > 0.85$ indicates super-case II transport.[67] According to the diffusional exponent parameters of Korsmeyer–Peppas, it has been found that there is Fickian diffusion in the release kinetics of the BRN9 formulation. This indicates that diffusion-based release from the polymeric scaffold, which forms the main structure of *in- situ* gel systems, is the dominant mechanism. In the Baker–Lonsdale model, which is the kinetic model to which the BRN9-CD formulation is compatible, the basic mechanism refers to the release from homogeneous polymeric matrix systems. It refers to dissolution-based release from permeable areas of the polymeric structure depending on the concentration gradient.[68,69] When evaluated from this perspective, it was determined that the diffusion-based release models were compatible in both formulations and the main mechanism in the release kinetics was diffusion in both formulations. The findings were evaluated in accordance with the literature and the diffusion-based drug release mechanisms from *in situ* gel systems were also confirmed with kinetic models.[70,71]

Hesperidin studies demonstrate that cell viability declines with concentration. According to studies on hesperidin's effects on cell viability published in the literature, cell viability declines as hesperidin concentration rises.[72] However, it was discovered that hesperidin had 73% cell viability at 400 g/mL, indicating that it is above the cytotoxic value in the literature.[73] Cell viability for drug-free, blank gel, and CD-blank gel appears to increase with increasing doses, indicating that our formulations enhance cell viability by increasing the metabolic activity and viability of cells and that the excipients used are not hazardous. Cell viability for drug-free, blank gel, and CD-blank gel appears to increase with increasing doses, suggesting that our formulations nourish and increase the vitality of cells and demonstrating that the excipients utilized are not hazardous. If the literature is considered, it can be found that the concentration of poloxamer increases with cell viability.[74,75] Hesperidin *in situ* gel has a higher level of cell viability than the hesperidin solution ($P < 0.01$). The formulation with the CD-hesperidin inclusion complex, however, has the maximum cell viability at each dose among the hesperidin-containing formulations. This is a result of the complex that cyclodextrin created. In MTT analyses for free drugs with inclusion complex, the literature shows that products containing inclusion complex have greater cell viability.[74] When the cell viability results of the blank gel were examined, it was observed that the cell viability results increased with concentration. In the blank gel and blank CD gel, cell viability was significantly increased at the highest concentration in comparison with other concentrations. This may be because poloxamer 407 increases cell proliferation by promoting metabolic activity and viability in L929 cells. There are examples in the literature where poloxamer 407 had higher cell viability than the control.[76] While cell viability was 73% when hesperidin was applied at a concentration of 400 μg/mL, cell viability was over 100% in cells treated with BRN9 and BRN9-CD formulations containing the same amount of hesperidin. This may be due to the fact that poloxamer 407 promotes cell viability and prevents the negative effects of high concentrations of hesperidin on cell viability.

The LOX enzymes contribute to the emergence of inflammation and allergic reactions through the production of leukotrienes.[77] Soybean LOX has similar substrate selectivity and inhibitory properties to human LOX, exhibits good stability, and is readily available from commercial sources, so it was used in a ferrous oxidation-xylenol orange (FOX) LOX inhibition assay.[78] In a previous study, a number of flavonoids were isolated from orange peel and their inhibitory activities against soybean 15-lipoxygenase were investigated, and hesperidin (180 ± 10 μM) was reported to show moderate activity inhibitory activity.[79] In another study, inclusion complexes (HP-*β*-CD) formed by hesperidin (HES) and (2-hydroxypropyl)-*β*-cyclodextrin were prepared and their ability to inhibit lipoxygenase activity was investigated by the modified Malterud method. As a result of the experiment, it was observed that HES included in the HP-*β*-CD cavity (IC_{50}: 0.0314 ± 0.33 Mm) showed a more significant lipoxygenase inhibition capacity than free HES (IC_{50}: 0.0565 ± 0.80 Mm).

This can be explained by the fact that the OH groups of HES and HP-*β*-CD block the iron ions involved in the redox reaction, and thus the oxidation of Fe^{2+} to Fe^{3+} does not occur, knowing that the action of the enzyme depends on the oxidation state of the iron.[80]

The modified Draize test results showed that none of the three substances tested caused any discomfort to the test rats' eyes (Figs 7(d) and 8). When the rats were inspected, it was discovered that their iris irritation and corneal opaqueness were both nearly nonexistent. It is therefore believed that the irritability of *in situ* gel is very low. Thus, we can say that the processing method did not affect the polymer's ability to transfer BRN9-CD to the ocular surface or its activity.[81] For the first time, *in situ* gel with

Journal of The Science of Food and Agriculture published by John Wiley & Sons Ltd on behalf of Society of Chemical Industry.

hesperidin-β-CD complex was developed for use in ocular system disorders. By reviewing the literature, it was found that the Draize tests conducted for non-steroidal anti-inflammatory drugs, which are believed to be utilized ocularly, may be appropriate for ocular usage with similar outcomes.[82,83]

CONCLUSION

Within the scope of the study, the hesperidin-CD inclusion complex was successfully produced by the freeze-drying method and demonstrated by DSC and FTIR analysis. Thermoresponsive ophthalmic *in situ* gels, which were fabricated with poloxamer P407 and HEC, were optimized and evaluated. The optimized formulations were further blended with the hesperidin or hesperidin-β-CD complex. It was discovered that the chosen formulation had temperature-responsive properties after looking at the gelling temperature and viscosities. As a result, the formulation's ocular application and occlusion time were at the anticipated levels. The chosen *in situ* thermosensitive gel formulation from this investigation had 1.5% (w/w) HEC as the gelling matrix and 16% (w/w) poloxamer as the polymer component. In release studies, BRN9 and BRN9-CD produced a burst release in the first 2 h, followed by an 8 h controlled release. However, in the release kinetic studies, it was determined that BRN9 was released in accordance with the Korsmeyer–Peppas model and BRN9-CD was in accordance with the Baker–Lonsdale model. The biocompatibility studies of the selected formulation loading the hesperidin or hesperidin-β-CD revealed that the formulation was acceptable for ophthalmic application. However, in the LOX inhibition study, hesperidin-β-CD showed an increased enzyme inhibition with increasing doses. The BRN9-CD optimized in this study demonstrates potential for application as an ocular delivery system with sustained drug release, corneal penetration, biocompatibility, *in vitro* anti-inflammatory studies and ocular irritation studies. Thus, hesperidin obtained from food industry waste and *in situ* thermosensitive gel (BRN9-CD) prepared from this hesperidin may be a promising formulation as an alternative for the treatment of ocular allergic disease. More animal and clinical research is needed, however, to evaluate the plausibility of its use in clinical practice.

ACKNOWLEDGEMENTS

This research did not receive any specific grant from funding agencies in the public, commercial, or not-for-profit sectors.

ETHICS COMMITTEE APPROVAL

Ethical committee approval was received from the Local Ethics Committee of Süleyman Demirel University Animal Experiments (Approval no: 155).

DATA AVAILABILITY STATEMENT

The data that supports the findings of this study are available in the supplementary material of this article.

SUPPORTING INFORMATION

Supporting information may be found in the online version of this article.

REFERENCES

1 Ma L and Lin XM, Effects of lutein and zeaxanthin on aspects of eye health. *J Sci Food Agric* **90**:2–12 (2010).
2 Trocme SD and Sra KK, Spectrum of ocular allergy. *Curr Opin Allergy Clin Immunol* **2**:423–427 (2002).
3 Calder J, Hingorani A, Leonardi S and Lightman B, Cytokine production and mRNA expression by conjunctival T-cell lines in chronic allergic eye disease. *Clin Exp Allergy* **29**:1214–1222 (1999).
4 Abelson MB, Chambers WA and Smith LM, Conjunctival allergen challenge: a clinical approach to studying allergic conjunctivitis. *Arch Ophthalmol* **108**:84–88 (1990).
5 Hingorani M, Calder V, Jolly G, Buckley RJ and Lightman SL, Eosinophil surface antigen expression and cytokine production vary in different ocular allergic diseases. *J Allergy Clin Immunol* **102**:821–830 (1998).
6 Mehl F, Marti G, Boccard J, Debrus B, Merle P, Delort E *et al.*, Differentiation of lemon essential oil based on volatile and non-volatile fractions with various analytical techniques: a metabolomic approach. *Food Chem* **143**:325–335 (2014).
7 Zhao C, Wang F, Lian Y, Xiao H and Zheng J, Biosynthesis of citrus flavonoids and their health effects. *Crit Rev Food Sci* **60**:566–583 (2020).
8 Rodríguez-Roque MJ, MaA R-G, Elez-Martínez P and Martín-Belloso O, Changes in vitamin C, phenolic, and carotenoid profiles throughout *in vitro* gastrointestinal digestion of a blended fruit juice. *J Agric Food Chem* **61**:1859–1867 (2013).
9 Gözcü S, Akşit Z, Şimşek S, Kandemir A, Aydın A, Yılmaz MA *et al.*, Phytochemical analysis and biological evaluation of *Ferulago setifolia* K. Koch. *J Agric Food Chem* **104**:1382–1390 (2024).
10 Hajialyani M, Hosein Farzaei M, Echeverría J, Nabavi SM, Uriarte E and Sobarzo-Sánchez E, Hesperidin as a neuroprotective agent: a review of animal and clinical evidence. *Molecules* **24**:648 (2019).
11 Mahmoud AM, Hernandez Bautista RJ, Sandhu MA and Hussein OE, Beneficial effects of citrus flavonoids on cardiovascular and metabolic health. *Oxid Med Cell Longev* **2019**:1–20 (2019).
12 Shehata AS, Amer MG, Abd El-Haleem MR and Karam RA, The ability of hesperidin compared to that of insulin for preventing osteoporosis induced by type I diabetes in young male albino rats: A histological and biochemical study. *Exp Toxicol Pathol* **69**:203–212 (2017).
13 Wang L, Li Y, He T, Cheng L, Zhou C and Zhou F, Hesperidin Exherts Antiglaucoma Effects by Activating Overexpression of BMP4 Signaling and Management of Retinal Ganglionic Cells Degeneration. *Curr Top Nutraceutical Res* **20**:505–512 (2022).
14 Hosawi S, Current Update on Role of Hesperidin in Inflammatory Lung Diseases: Chemistry, Pharmacology, and Drug Delivery Approaches. *Life* **13**:937 (2023).
15 Rekha SS, Pradeepkiran JA and Bhaskar M, Bioflavonoid hesperidin possesses the anti-hyperglycemic and hypolipidemic property in STZ induced diabetic myocardial infarction (DMI) in male Wister rats. *J Nutr Intermed Metab* **15**:58–64 (2019).
16 Bilginer S, Gözcü S and Güvenalp Z, Molecular Docking Study of Several Seconder Metabolites from Medicinal Plants as Potential Inhibitors of COVID-19 Main Protease. *Turk J Pharm Sci* **19**:431 (2022).
17 Huang Y, Zhou W, Sun J and Ou G, Zhong N—S and Liu Z, Exploring the potential pharmacological mechanism of hesperidin and glucosyl hesperidin against COVID-19 based on bioinformatics analyses and antiviral assays. *Am J Chinese Med* **50**:351–369 (2022).
18 Kilic K, Sakat MS, Yildirim S, Kandemir FM, Gozeler MS, Dortbudak MB *et al.*, The amendatory effect of hesperidin and thymol in allergic rhinitis: an ovalbumin-induced rat model. *Eur Arch Oto-Rhino-L* **276**:407–415 (2019).
19 Choi IY, Kim SJ, Jeong HJ, Park SH, Song YS, Lee JH *et al.*, Hwang GS and Lee E-, Hesperidin inhibits expression of hypoxia inducible factor-1 alpha and inflammatory cytokine production from mast cells. *Mol Cell Biochem* **305**:153–161 (2007).
20 Srirangam R, Hippalgaonkar K, Avula B, Khan IA and Majumdar S, Evaluation of the intravenous and topical routes for ocular delivery of hesperidin and hesperetin. *J Ocul Pharmacol Ther* **28**:618–627 (2012).
21 Deshetty UM, Tamatam A, Bhattacharjee M, Perumal E, Natarajan G and Khanum F, Ameliorative effect of hesperidin against motion sickness by modulating histamine and histamine H1 receptor expression. *Neurochem Res* **45**:371–384 (2020).
22 Lee NK, Choi SH, Park SH, Park EK and Kim DH, Antiallergic activity of hesperidin is activated by intestinal microflora. *Pharmacology* **71**:174–180 (2004).

23 Garg A, Garg S, Zaneveld L and Singla A, Chemistry and pharmacology of the citrus bioflavonoid hesperidin. *Phytother Res* **15**:655–669 (2001).
24 Majumdar S and Srirangam R, Solubility, stability, physicochemical characteristics and *in vitro* ocular tissue permeability of hesperidin: a natural bioflavonoid. *Pharm Res* **26**:1217–1225 (2009).
25 Polat H, *In situ* gels triggered by temperature for ocular delivery of dexamethasone and dexamethasone/SBE-*β*-CD complex. *J Res Pharm* **26**:873–883 (2022).
26 Polat HK, Kurt N, Aytekin E, Bozdağ Pehlivan S and Çalış S, Novel drug delivery systems to improve the treatment of keratitis. *J Ocul Pharmacol Ther* **38**:376–395 (2022).
27 Ma Q, Luo R, Zhang H, Dai M, Bai L, Fei Q *et al*., Design, characterization, and application of a pH-triggered *in situ* gel for ocular delivery of vinpocetine. *AAPS PharmSciTech* **21**:1–11 (2020).
28 Youssef AAA, Dudhipala N and Majumdar S, Dual drug loaded lipid nanocarrier formulations for topical ocular applications. *Int J Nanomedicine* **17**:2283–2299 (2022).
29 Ünal S, Polat H, Yuvalı D and Köngül Şafak E, Development of *in situ* gel containing CUR: HP-*β*-CD inclusion complex prepared for ocular diseases: Formulation, characterization, anti-inflammatory, anti-oxidant evaluation and comprehensive release kinetic studies. *J Res Pharm* **27**:97–119 (2023).
30 Polat HK, Design of Metformin HCl and Moxifloxacin HCl Loaded Thermosensitive *In Situ* Gel. *J Res Pharm* **26**:1230–1241 (2022).
31 Sharma P, Pandey P, Gupta R, Roshan S, Garg A, Shulka A *et al*., Isolation and characterization of hesperidin from orange peel. *J Pharm Res* **3**:3892–3897 (2013).
32 Lahmer N, Belboukhari N, Cheriti A and Sekkoum K, Hesperidin and hesperitin preparation and purification from *Citrus sinensis* peels. *Der Pharma Chem* **7**:1–4 (2015).
33 Loftsson T and Brewster ME, Pharmaceutical applications of cyclodextrins: basic science and product development. *J Pharm Pharmacol* **62**:1607–1621 (2010).
34 Lu B, Wang X, Ren Z, Jiang H and Liu B, Anti-glaucoma potential of hesperidin in experimental glaucoma induced rats. *AMB Express* **10**:1–6 (2020).
35 Polat HK, Pehlivan SB, Özkul C, Çalamak S, Öztürk N, Aytekin E *et al*., Development of besifloxacin HCl loaded nanofibrous ocular inserts for the treatment of bacterial keratitis: *In vitro*, *ex vivo* and *in vivo* evaluation. *Int J Pharm* **585**:119552 (2020).
36 Fathalla ZM, Vangala A, Longman M, Khaled KA, Hussein AK, El-Garhy OH *et al*., Poloxamer-based thermoresponsive ketorolac tromethamine *in situ* gel preparations: Design, characterisation, toxicity and transcorneal permeation studies. *Eur J Pharm Biopharm* **114**: 119–134 (2017).
37 Obiedallah MM, Abdel-Mageed A and Elfaham TH, Ocular administration of acetazolamide microsponges *in situ* gel formulations. *Saudi Pharm J* **26**:909–920 (2018).
38 El-Feky YA, Fares AR, Zayed G, El-Telbany RFA, Ahmed KA and El-Telbany DFA, Repurposing of nifedipine loaded *in situ* ophthalmic gel as a novel approach for glaucoma treatment. *Biomed Pharmacother* **142**:112008 (2021).
39 Zhang Y, Huo M, Zhou J, Zou A, Li W, Yao C *et al*., DDSolver: an add-in program for modeling and comparison of drug dissolution profiles. *The AAPS journal* **12**:263–271 (2010).
40 Usta DY, Demirtaş Ö, Ökçelik C, Abdullah U and Teksin ZŞ, Evaluation of *in vitro* dissolution characteristics of flurbiprofen, a BCS class IIa drug. *Fabad J. Pharm. Sci* **43**:117–124 (2018).
41 Yu J, Xu X, Yao F, Luo Z, Jin L, Xie B *et al*., *In situ* covalently cross-linked PEG hydrogel for ocular drug delivery applications. *Int. J. Pharm* **470**: 151–157 (2014).
42 Aksungur P, Demirbilek M, Denkbaş EB, Vandervoort J, Ludwig A and Ünlü N, Development and characterization of Cyclosporine A loaded nanoparticles for ocular drug delivery: Cellular toxicity, uptake, and kinetic studies. *J Control Release* **151**:286–294 (2011).
43 Waslidge NB and Hayes DJ, A colorimetric method for the determination of lipoxygenase activity suitable for use in a high throughput assay format. *Anal. Biochem* **231**:354–358 (1995).
44 Chung LY, Soo WK, Chan KY, Mustafa MR, Goh SH and Imiyabir Z, Lipoxygenase inhibiting activity of some Malaysian plants. *Pharm Biol* **47**: 1142–1148 (2009).
45 Wilhelmus KR, The Draize eye test. *Surv. Ophthalmol* **45**:493–515 (2001).
46 Alpay A, Evren C, Bektaş S, Ugurbas SC, Ugurbas SH and Çınar F, Effects of the folk medicinal plant extract Ankaferd Blood Stopper® on the ocular surface. *Cutan Ocul Toxicol* **30**:280–285 (2011).
47 Abdelkader H, Pierscionek B and Alany RG, Novel *in situ* gelling ocular films for the opioid growth factor-receptor antagonist-naltrexone hydrochloride: Fabrication, mechanical properties, mucoadhesion, tolerability and stability studies. *Int J Pharm* **477**:631–642 (2014).
48 Pignatello R, Bucolo C, Spedalieri G, Maltese A and Puglisi G, Flurbiprofen-loaded acrylate polymer nanosuspensions for ophthalmic application. *Biomaterials* **23**:3247–3255 (2002).
49 Karayıldırım ÇK, Characterization and *in vitro* evolution of antibacterial efficacy of novel hesperidin microemulsion. *CBUJOS* **13**:943–947 (2017).
50 Polat HK, Kurt N, Aytekin E, Akdağ Çaylı Y, Bozdağ Pehlivan S and Çalış S, Design of besifloxacin HCl-loaded nanostructured lipid carriers: *in vitro* and *ex vivo* evaluation. *J Ocul Pharmacol Ther* **38**:412–423 (2022).
51 Venkatesh D, Kamlesh L and Kumar P, Development and evaluation of chitosan based thermosensitive *in situ* gels of pilocarpine. *Int J Pharm Pharmaceut Sci* **5**:164–169 (2013).
52 Lanier OL, Manfre MG, Bailey C, Liu Z, Sparks Z, Kulkarni S *et al*., Review of approaches for increasing ophthalmic bioavailability for eye drop formulations. *Aaps Pharmscitech* **22**:1–16 (2021).
53 Han H, Li S, Xu M, Zhong Y, Fan W, Xu J *et al*., Polymer-and lipid-based nanocarriers for ocular drug delivery: Current status and future perspectives. *Adv Drug Deliv Rev* **114**:770 (2023).
54 Burton MJ, Ramke J, Marques AP, Bourne RR, Congdon N, Jones I *et al*., The Lancet global health Commission on global eye health: vision beyond 2020. *Lancet Glob. Health* **9**:e489–e551 (2021).
55 Cao R, Zhao Y, Zhou Z and Zhao X, Enhancement of the water solubility and antioxidant activity of hesperidin by chitooligosaccharide. *J Sci Food Agric* **98**:2422–2427 (2018).
56 Dillard CJ and German JB, Phytochemicals: nutraceuticals and human health. *J Sci Food Agric* **80**:1744–1756 (2000).
57 Simitzis PE, Charismiadou MA, Goliomytis M, Charalambous A, Ntetska I, Giamouri E *et al*., Antioxidant status, meat oxidative stability and quality characteristics of lambs fed with hesperidin, naringin or *α*-tocopheryl acetate supplemented diets. *J Sci Food Agric* **99**:343–349 (2019).
58 Patel A, Cholkar K, Agrahari V and Mitra AK, Ocular drug delivery systems: An overview. *World J Pharmacol* **2**:47 (2013).
59 Cabana A, Aït-Kadi A and Juhász J, Study of the gelation process of polyethylene oxidea–polypropylene oxideb–polyethylene oxideacopolymer (poloxamer 407) aqueous solutions. *J. Colloid Interface Sci* **190**:307–312 (1997).
60 Okur NÜ, Yozgatlı V and Şenyiğit Z, Formulation and detailed characterization of voriconazole loaded *in situ* gels for ocular application. *J Fac Pharm Ankara* **44**:33–49 (2020).
61 Polat HK, Arslan A, Ünal S, Haydar MK, Aytekin E, Gözcü S *et al*., Formulation Development of Dual Drug-Loaded Thermosensitive Ocular *In Situ* Gel Using Factorial Design. *J Pharm Innov* **18**:768–788 (2023).
62 Sharif N, Golmakani MT, Niakousari M, Hosseini SMH, Ghorani B and Lopez-Rubio A, Active food packaging coatings based on hybrid electrospun gliadin nanofibers containing ferulic acid/hydroxypropyl-beta-cyclodextrin inclusion complexes. *Nanomaterials* **8**:919 (2018).
63 Supramaniam J, Adnan R, Kaus NHM and Bushra R, Magnetic nanocellulose alginate hydrogel beads as potential drug delivery system. *Int J Biol Macromol* **118**:640–648 (2018).
64 Tajani AS, Haghighizadeh A, Soheili V, Mirshahi S and Rajabi O, *In vitro* bioequivalence study of 8 generic and 3 brands of sertraline-HCl tablets in Iran market. *Biomed. Pharmacol. J.* **10**:1109–1116 (2017).
65 Trucillo P, Drug carriers: A review on the most used mathematical models for drug release. *Processes* **10**:1094 (2022).
66 Ünal S, Varan G, Benito JM, Aktaş Y and Bilensoy E, Insight into oral amphiphilic cyclodextrin nanoparticles for colorectal cancer: comprehensive mathematical model of drug release kinetic studies and antitumoral efficacy in 3D spheroid colon tumors. *Beilstein J Organic Chem* **19**:139–157 (2023).
67 Ünal S and Aktaş Y, Bisphosphonate-loaded PLGA microspheres for bone regeneration in dental surgery: formulation, characterization, stability, and comprehensive release kinetic studies. *Int J Polym Mater* **72**:89–100 (2023).
68 Talevi A and Bellera CL eds, Biopharmaceutics drug disposition classification system, in *The ADME Encyclopedia: A Comprehensive Guide on Biopharmacy and Pharmacokinetics*, 1st edn. Springer, Cham (2022).

69 Ge M, Li X, Li Y, Jahangir Alam S, Gui Y, Huang Y *et al*., Preparation of Magadiite-Sodium Alginate Drug Carrier Composite by Pickering-Emulsion-Templated-Encapsulation Method and Its Properties of Sustained Release Mechanism by Baker–Lonsdale and Korsmeyer–Peppas Model. *J Polym Environ* **30**:3890–3900 (2022).

70 Pandya K, Aggarwal P, Dashora A, Sahu D, Garg R, Pareta LK *et al*., Formulation and evaluation of oral floatable *in situ* gel of ranitedine hydrochloride. *J drug deliv ther* **3**:90–97 (2013).

71 Vijaya Rani KR, Rajan S, Bhupathyraaj M, Priya RK, Halligudi N, Al-Ghazali MA *et al*., The effect of polymers on drug release kinetics in nanoemulsion *in situ* gel formulation. *Polymers* **14**:427 (2022).

72 Sulaiman GM, Waheeb HM, Jabir MS, Khazaal SH, Dewir YH and Naidoo Y, Hesperidin loaded on gold nanoparticles as a drug delivery system for a successful biocompatible, anti-cancer, anti-inflammatory and phagocytosis inducer model. *Sci Rep* **10**:9362 (2020).

73 Pezik E, Gulsun T, Sahin S and Vural I, Development and characterization of pullulan-based orally disintegrating films containing amlodipine besylate. *Eur J Pharm Sci* **156**:105597 (2021).

74 Wangsawangrung N, Choipang C, Chaiarwut S, Ekabutr P, Suwantong O, Chuysinuan P *et al*., Quercetin/Hydroxypropyl-β-Cyclodextrin Inclusion Complex-Loaded Hydrogels for Accelerated Wound Healing. *Gels* **8**:573 (2022).

75 Samimi M, Mahboobian M and Mohammadi M, Ocular toxicity assessment of nanoemulsion *in situ* gel formulation of fluconazole. *Hum Exp Toxicol* **40**:2039–2047 (2021).

76 Niyompanich J, Chuysinuan P, Pavasant P and Supaphol P, Development of thermoresponsive poloxamer *in situ* gel loaded with gentamicin sulfate for cavity wounds. *J Polym Res* **28**:1–13 (2021).

77 Alam F and Ashraf M, Phenolic contents, elemental analysis, antioxidant and lipoxygenase inhibitory activities of *Zanthoxylum armatum* DC fruit, leaves and bark extracts. *Pak J Pharm Sci* **32** :1703-1708 (2019).

78 Chan KY, Mohamad K, Ooi AJ, Imiyabir Z and Chung LY, Bioactivity-guided fractionation of the lipoxygenase and cyclooxygenase inhibiting constituents from *Chisocheton polyandrus* Merr. *Fitoterapia* **83**:961–967 (2012).

79 Malterud KE and Rydland KM, Inhibitors of 15-lipoxygenase from orange peel. *J Agric Food Chem* **48**:5576–5580 (2000).

80 Corciova A, Ciobanu C, Poiata A, Nicolescu A, Drobota M, Varganici C *et al*., Inclusion complexes of hesperidin with hydroxypropyl-β-cyclodextrin. Physico-chemical characterization and biological assessment. *Dig J Nanomater Biostruct* **9**:1623–1637 (2014).

81 Pokharkar V, Patil V and Mandpe L, Engineering of polymer–surfactant nanoparticles of doxycycline hydrochloride for ocular drug delivery. *Drug Deliv* **22**:955–968 (2015).

82 Agnihotri SM and Vavia PR, Diclofenac-loaded biopolymeric nanosuspensions for ophthalmic application. *Nanomedicine* **5**:90–95 (2009).

83 Gonzalez-Mira E, Egea M, Garcia M and Souto E, Design and ocular tolerance of flurbiprofen loaded ultrasound-engineered NLC. *Colloids Surf* **81**:412–421 (2010).

